J. Fluid Mech. (2007), *vol.* 586, *pp.* 491–506.
doi:10.1017/S0022112007007252 Printed in the United Kingdom

Free convection beneath a heated horizontal plate in a rapidly rotating system

ROBERT J. WHITTAKER† AND JOHN R. LISTER

Institute of Theoretical Geophysics, Department of Applied Mathematics and Theoretical Physics, University of Cambridge, Wilberforce Road, Cambridge, CB3 0WA, UK

(Received 10 March 2006 and in revised form 3 May 2007)

Laminar flow beneath a finite heated horizontal plate in a rapidly rotating system is considered in both axisymmetric and planar geometries. In particular, we examine the case where the Ekman layer is confined well within a much deeper (yet still thin) thermal boundary layer. This situation corresponds to the regime $E^{-3/2} \ll Ra \ll E^{-5/2}$, where E and Ra are the natural Ekman and Rayleigh numbers for the system (equation (2.6)). The outward flux of buoyant fluid from beneath the plate occurs primarily in the Ekman layer, while outward flow in the thicker thermal boundary layer is inhibited by a dominant thermal-wind balance. The $O(Ra^{-1/2}E^{-3/4})$ thickness of the thermal boundary layer is determined by a balance between Ekman suction and diffusion. There are several possible asymptotic regimes near the outer edge of the plate, differing only by logarithmic factors, but in all cases the edge corresponds to a simple boundary condition on the interior flow. With a uniform plate temperature, the dimensionless heat transfer (equation (7.6)) is given by a Nusselt number $Nu \sim \frac{1}{2}Ra^{1/2}E^{3/4}[\ln(Ra^{-1}E^{-5/2})]^{1/2}$. The solution for a uniform plate heat flux is also presented.

1. Introduction

The flow that develops beneath a finite heated horizontal plate is a fundamental problem in natural convection. The heating creates a pool of buoyant fluid directly beneath the plate. Owing to drainage of this fluid at the edge, the pool is thicker in the middle, and the resulting horizontal pressure gradient drives the fluid outwards.

The non-rotating case has been studied extensively over a wide range of Prandtl numbers. For example, experiments (Aihara, Yamada & Endo 1972; Hatfield & Edwards 1981), numerical simulations (Goldstein & Lau 1983), and theoretical investigations (Singh & Birkebak 1969; Higuera 1993) have all been reported. For sufficiently large Rayleigh numbers, the thermal boundary layer is thin compared with the horizontal scale of the plate. Boundary-layer approximations can be employed, and reveal that the Nusselt number for the heat transfer from a uniform-temperature plate scales like $Nu \sim Ra^{1/5}$, where Ra is a Rayleigh number based on the size of the plate. Formal definitions of Ra and Nu are given in (2.6) and (7.6) respectively.

In contrast, we are not aware of any comparable studies of this type of convection in a rapidly rotating system. Imposed thermal variations on the top surface of a rotating cylinder have previously been considered by Pedlosky, Whitehead & Veitch (1997).

† Present address: Centre for Mathematical Medicine and Biology, School of Mathematical Sciences, University of Nottingham, University Park, Nottingham, NG7 2RD, UK.

However, this study dealt with linear perturbations to a background stratification, and was of an enclosed cylinder. Other studies of convection in a rotating system have considered sidewall heating (e.g. Hunter 1967; McIntyre 1968), or the case where the buoyancy force is directed away from the horizontal surface at which the thermal forcing is applied (e.g. Boubnov & Fernando 1999).

In this short paper, we study the simple problem of steady convection in rapid rotation from beneath a heated horizontal plate — either a circular disk, or an infinite strip. As in the non-rotating case, there is a buoyant layer and an outward pressure gradient, but now most of the outflow is expected to be confined to a thin Ekman layer. We focus our attention on the case where this Ekman layer is thin compared with the thermal boundary layer,† which in turn is much thinner than the horizontal scale of the plate. The parameter regime in which this holds is identified, and we present the solutions for conditions of uniform temperature and of uniform heat flux on the plate. The assumption of steady flow allows analytical understanding of the scalings and dominant balances in the flow under the plate and near the edge, and can partly be motivated by the experimental observations by Pedlosky *et al.* (1997) of steady flow in a related problem. Nevertheless, the possibility of unsteady flow cannot immediately be discounted and, as discussed briefly in § 9, it would thus be desirable to examine the stability of the steady solutions derived here in future numerical or experimental work.

As well as being a classical problem in its own right, this study of convection beneath a heated rotating plate represents a first step towards understanding a possible flow in the Earth's fluid outer core just below the core–mantle boundary. Since the mantle convects much more sluggishly than the core (by a factor of order 10^6), it imposes a quasi-steady, but spatially variable, heat-flux boundary condition on the core flow, which influences the Earth's magnetic field (see e.g. Bloxham & Gubbins 1987; Kohler & Stevenson 1990; Zhang & Gubbins 1992; Olson & Glatzmaier 1996; Sarson, Jones & Longbottom 1997; Gibbons & Gubbins 2000; Olson & Christensen 2002). One issue in such modelling is whether, and by how much, the imposed heat flux is sub-adiabatic or super-adiabatic with respect to the core adiabat. For example, if the heat flux is everywhere sub-adiabatic then a global thermally stratified layer can form at the top of the core (e.g. Labrosse, Poirier & Le Mouël 1997; Lister & Buffett 1998). In contrast, if the flux is only locally sub-adiabatic, as seems much more likely, then local stratified patches can form just below the core–mantle boundary (Olson & Glatzmaier 1996) and spread laterally towards the bounding adjacent regions of super-adiabatic convection. This spread is loosely analogous to the lateral spread of the buoyant layer below a heated plate analysed herein, though we note that magnetic braking plays a significant role in flows near the core–mantle boundary (e.g. Lister 2004) and that a finite plate edge is not the same as bounding adjacent convection. Nevertheless, the simple problem of a heated plate allows an initial exploration of the balance between diffusive thickening and rotationally inhibited lateral drainage. From a theoretical point of view, we observe that laterally driven flow with rapid rotation has a different asymptotic structure from, for example, the marginal convection states in a rapidly rotating spherical annulus (e.g. Roberts 1968; Busse 1970; Jones, Soward

† The alternative limit, in which the thermal boundary layer is much thinner than the Ekman layer, reduces to the non-rotating case, as the thermal boundary layer is then not significantly affected by the rotation. When the layer depths are comparable the problem requires numerical solution.

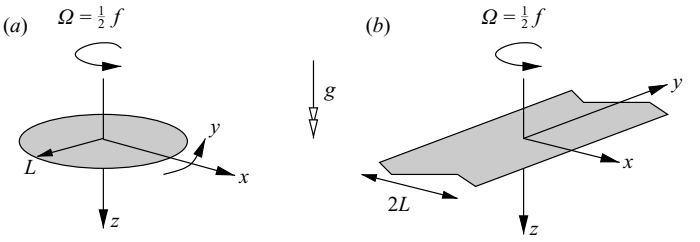

FIGURE 1. An overview of the two geometries being considered, showing a circular disk (*a*) and a rectangular strip (*b*). Note the left-handed coordinate system, but with the rotation vector oriented in the direction of $-\hat{\boldsymbol{e}}_z$.

& Musse 2000; Dormy *et al.* 2003), which are driven by net radial heat flow and dominated by cylindrical rolls around the tangent cylinder.

The problem to be solved is described and the scalings presented in § 2. The asymptotic solution for a uniform plate temperature is constructed in §§ 3–6 and the adaptations for a uniform heat flux outlined in § 8. The detailed asymptotic structure near the plate edge is discussed in § 7 and the Appendix. Our conclusions are summarized in § 9.

2. Problem description

2.1. *Governing equations*

We consider the flow beneath a horizontal plate of half-width L, held at a constant temperature ΔT above the temperature T_0 of the ambient fluid. (See § 8 for the case of a uniform heat flux.) The plate is either a strip that is infinite in the y-direction and has width $2L$ in the x-direction, or a circular disk of radius L for which we let x denote the radial coordinate and y the azimuthal coordinate. In both cases we let z denote the downward distance from the surface of the plate, $g\hat{\boldsymbol{e}}_z$ the acceleration due to gravity, and $-\frac{1}{2}f\hat{\boldsymbol{e}}_z$ the rotation vector. See figure 1. We denote the velocity components by (u, v, w) and the pressure by p, and seek solutions in which the flow is assumed to be steady and independent of y.

We employ the Boussinesq approximation, and assume that the kinematic viscosity ν, thermal diffusivity κ, and thermal expansivity β are all independent of the temperature T. Conservation of mass implies that

$$\frac{1}{x^\ell}\frac{\partial}{\partial x}(x^\ell u) + \frac{\partial w}{\partial z} = 0, \tag{2.1}$$

where $\ell = 0$ when the heated region is an infinite strip, and $\ell = 1$ when it is a circular disk. Neglecting the centrifugal term (assuming that $Lf^2/g \ll 1$), the components of the momentum equation are

$$u\frac{\partial u}{\partial x} + w\frac{\partial u}{\partial z} - fv = -\frac{1}{\rho_0}\frac{\partial p}{\partial x} + \nu\left(\nabla^2 u - \frac{\ell u}{x^2}\right), \tag{2.2}$$

$$u\frac{\partial v}{\partial x} + w\frac{\partial v}{\partial z} + fu = \nu\left(\nabla^2 v - \frac{\ell v}{x^2}\right), \tag{2.3}$$

$$u\frac{\partial w}{\partial x} + w\frac{\partial w}{\partial z} = -\frac{1}{\rho_0}\frac{\partial p}{\partial z} + g[1 - \beta(T - T_0)] + \nu\nabla^2 w. \tag{2.4}$$

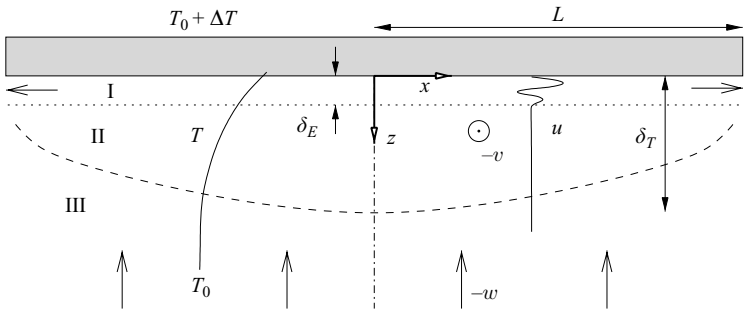

FIGURE 2. A sketch showing the expected form of the flow, with three distinct regions: the inner Ekman layer (I), the geostrophic thermal boundary layer (II), and the bulk fluid (III).

Finally, the heat equation is

$$u\frac{\partial T}{\partial x} + w\frac{\partial T}{\partial z} = \kappa\nabla^2 T. \tag{2.5}$$

The boundary conditions on these equations are described later. The dimensionless parameters are the Rayleigh, Ekman and Prandtl numbers,

$$Ra = \frac{g\beta\Delta T L^3}{\nu\kappa}, \qquad E = \frac{2\nu}{fL^2}, \qquad Pr = \frac{\nu}{\kappa}. \tag{2.6}$$

2.2. *Regions and scalings*

Figure 2 shows the anticipated form of the flow beneath the heated plate. The non-uniform thickness of the thermal boundary layer sets up a horizontal pressure gradient below the plate. This drives an outward flux in an Ekman layer (region I) of thickness $\delta_E \sim LE^{1/2}$. The remainder of the thermal boundary layer (region II, typical thickness δ_T) is in geostrophic balance at leading order, so that the pressure gradient drives a transverse thermal wind v rather than any significant outward flow u.

The divergence of the flux in the Ekman layer sucks fluid up from below, so there is a small vertical velocity w throughout the thermal boundary layer. This velocity also penetrates deep into the bulk fluid (region III) by virtue of the Taylor–Proudman constraint. Since the geostrophic velocity is divergence-free, w is a function only of x in region II. This vertical velocity sets up an advection–diffusion balance that determines the thickness of the thermal boundary layer, and thus closes the problem for $x < L$.

Since the boundary layers are thin and the flows mainly horizontal, we expect the vertical pressure gradient to be hydrostatic. Hence

$$p - p_0 - \rho_0 g z \sim \rho_0 g\beta\,\Delta T\,\delta_T. \tag{2.7}$$

Balancing the viscous, Coriolis and pressure forces in the Ekman layer gives

$$(u, v)\frac{\nu}{\delta_E^2} \sim (fu, fv) \sim \frac{\partial p}{\partial x}. \tag{2.8}$$

The scaling $fv \sim \partial p/\partial x$ also applies in the thermal boundary layer and corresponds to a thermal-wind balance.

Balancing the Ekman flux with the vertical mass flux, we obtain

$$w\,L \sim u\,\delta_E. \tag{2.9}$$

Finally, an advection–diffusion balance in region II sets the scale for the thermal boundary layer as

$$\delta_T \sim \frac{\kappa}{w}. \tag{2.10}$$

Combining these scaling estimates, we define dimensionless coordinates

$$X = \frac{x}{L}, \qquad Y = \frac{y}{L}, \qquad Z = \frac{z}{\delta_T}, \qquad \zeta = \frac{z}{\delta_E}, \tag{2.11}$$

where

$$\delta_T = L\,Ra^{-1/2}\,E^{-3/4} \quad \text{and} \quad \delta_E = LE^{1/2}. \tag{2.12}$$

For the vertical coordinate, ζ will be used in the Ekman layer (region I) and Z will be used in the thermal boundary layer (region II). We also define dimensionless dependent variables by

$$(u, v, w) = \frac{\kappa}{L} Ra^{1/2} E^{1/4} \left(U, V, E^{1/2}\, W\right), \tag{2.13}$$

$$p - p_0 - \rho_0 g z = \rho_0 g \beta \Delta T\, L\, Ra^{-1/2} E^{-3/4}\, P, \tag{2.14}$$

$$T - T_0 = \Delta T\, \theta. \tag{2.15}$$

Outside the Ekman layer, the lack of a pressure gradient in the y-direction implies that the dominant velocity in the x-direction is due to ageostrophic corrections, and is much smaller than the thermal wind in the y-direction. We estimate $u \sim vv/f\delta_T^2$, which leads to a revised scaling of

$$u(x, z) = \frac{\kappa}{L} Ra^{3/2} E^{11/4}\, U_a(X, Z) \tag{2.16}$$

in region II.

The scaled variables are substituted into the governing equations (2.1)–(2.5). In order to obtain the leading-order balances anticipated above, the boundary-layer scales must be well separated, i.e.

$$\delta_E \ll \delta_T \ll L \quad \Leftrightarrow \quad E^{-3/4} \ll Ra^{1/2} \ll E^{-5/4}. \tag{2.17}$$

Physically, the convective flow must be sufficiently large to allow confinement of the thermal buoyancy to a thin boundary layer, but not so large that the thickness of the thermal boundary layer becomes as small as that of the Ekman layer.

For simplicity, we also assume that $Pr \geqslant O(1)$, which ensures that inertial terms do not appear prematurely in various places and further complicate the asymptotic analysis.

3. The Ekman layer

In terms of the scaled variables defined in (2.11)–(2.15), the leading-order equations within the Ekman layer are

$$\frac{\partial W}{\partial \zeta} = -\frac{1}{X^\ell} \frac{\partial}{\partial X}(X^\ell U), \tag{3.1}$$

$$2V = \frac{\partial P}{\partial X} - \frac{\partial^2 U}{\partial \zeta^2}, \tag{3.2}$$

$$2U = \frac{\partial^2 V}{\partial \zeta^2}, \tag{3.3}$$

$$\frac{\partial P}{\partial \zeta} = O\left(Ra^{1/2}E^{5/4}\right), \tag{3.4}$$

$$\frac{\partial^2 \theta}{\partial \zeta^2} = Ra^{1/2}E^{5/4}\left(U\frac{\partial \theta}{\partial X} + W\frac{\partial \theta}{\partial \zeta}\right). \tag{3.5}$$

The boundary conditions are that the velocities vanish and $\theta = 1$ on $\zeta = 0$, and that the velocities, pressure and temperature match those in the thermal boundary layer as $\zeta \to \infty$.

Equations (3.5) and (2.17) show that the vertical variation in $\partial\theta/\partial\zeta$ across the Ekman layer is small. Since $\partial\theta/\partial\zeta$ must be matched below to the thermal boundary layer, which has a much larger vertical scale, we can therefore expect $\partial\theta/\partial\zeta$ to be small throughout the Ekman layer. Applying the boundary condition at $\zeta = 0$, we conclude that, at leading order,

$$\theta(X, \zeta) = 1 \tag{3.6}$$

throughout the Ekman layer. We also note in passing that the right-hand side of (3.5) is much smaller than the apparent $Ra^{1/2}E^{5/4}$ scaling, so that the change in $\partial\theta/\partial\zeta$ is negligible (in the sense that it is much smaller than its typical magnitude) across the Ekman layer.

From (3.4), the pressure is vertically uniform within the Ekman layer, so we write

$$P(X, \zeta) = P_0(X), \tag{3.7}$$

where P_0 is imposed by the pressure in the thermal boundary layer as $Z \to 0$.

The remaining equations (3.1)–(3.3) give rise to a standard Ekman-layer flow, with an outwards flux driven by the horizontal gradient of the, as yet unknown, pressure $P_0(X)$. The horizontal velocities are given by

$$(U, V) = -\frac{1}{2}\frac{\mathrm{d}P_0}{\mathrm{d}X}(\sin\zeta\,\mathrm{e}^{-\zeta},\ \cos\zeta\,\mathrm{e}^{-\zeta} - 1) \tag{3.8}$$

and, by continuity, the vertical velocity is

$$W(X, \zeta) = \frac{1}{4X^{\ell}}\frac{\mathrm{d}}{\mathrm{d}X}\left(X^{\ell}\frac{\mathrm{d}P_0}{\mathrm{d}X}\right)[1 - (\cos\zeta + \sin\zeta)\mathrm{e}^{-\zeta}]. \tag{3.9}$$

4. The thermal boundary layer

The leading-order balances in (2.1)–(2.5) within the thermal boundary layer are

$$\frac{\partial W}{\partial Z} = 0, \tag{4.1}$$

$$2V = \frac{\partial P}{\partial X}, \tag{4.2}$$

$$2U_a = \frac{\partial^2 V}{\partial Z^2} - Pr^{-1}W\frac{\partial V}{\partial Z}, \tag{4.3}$$

$$\frac{\partial P}{\partial Z} = -\theta, \tag{4.4}$$

$$W\frac{\partial \theta}{\partial Z} = \frac{\partial^2 \theta}{\partial Z^2}. \tag{4.5}$$

The boundary conditions are obtained by matching to the Ekman layer as $Z \to 0$ and to some sort of bulk flow as $Z \to \infty$.

Noting from (4.1) that $W = W(X)$, we solve (4.5) to obtain

$$\theta(X, Z) = \theta_0(X)\,\mathrm{e}^{-Z/H(X)}, \tag{4.6}$$

where we have written

$$W(X) = -\frac{1}{H(X)} \tag{4.7}$$

to introduce the thickness $H(X)$ of the thermal boundary layer, and $\theta_0(X)$ is the temperature to be matched with the Ekman layer. (Clearly $\theta_0 = 1$ for the fixed-temperature problem, but this notation proves convenient for the fixed-flux problem in § 8.) We now integrate (4.4) to obtain

$$P(X, Z) = \theta_0(X)\,H(X)\,\mathrm{e}^{-Z/H(X)} + P_\infty(X), \tag{4.8}$$

where $P_\infty(X)$ is given by matching as $Z \to \infty$. From (4.2), the horizontal pressure gradient induces a thermal wind

$$V = \frac{1}{2}\frac{\mathrm{d}H}{\mathrm{d}X}\left(1 + \frac{Z}{H}\right)\mathrm{e}^{-Z/H} + \frac{1}{2}\frac{\mathrm{d}P_\infty}{\mathrm{d}X}. \tag{4.9}$$

Finally, (4.3) determines the much smaller ageostrophic outward velocity

$$U_a = \frac{1}{4H^2}\frac{\mathrm{d}H}{\mathrm{d}X}\left(1 - Pr^{-1} - \frac{Z}{H}\right)\mathrm{e}^{-Z/H}. \tag{4.10}$$

Equations (4.6)–(4.10) describe the solution in the thermal boundary layer in terms of the functions $\theta_0(X)$, $H(X)$, and $P_\infty(X)$, which are determined by matching.

5. Matching

5.1. *Matching between the Ekman and thermal boundary layers*

Matching the pressure P between the Ekman layer and the thermal boundary layer leads to

$$P_0 = \theta_0 H + P_\infty. \tag{5.1}$$

Matching the vertical velocity $W = -1/H$ to (3.9) leads to

$$\frac{1}{4X^\ell}\frac{\mathrm{d}}{\mathrm{d}X}\left(X^\ell\frac{\mathrm{d}P_0}{\mathrm{d}X}\right) + \frac{1}{H} = 0. \tag{5.2}$$

Matching the temperature θ leads to $\theta_0(X) = 1$.

The transverse velocity V matches automatically (owing to the matching of P), and the outward velocity U does not need to be matched at this order since it decays to zero towards the base of the Ekman layer, and U_a has a much smaller scale in the thermal boundary layer.

Eliminating P_0 and θ_0, we obtain

$$\frac{1}{X^\ell}\frac{\mathrm{d}}{\mathrm{d}X}\left[X^\ell\left(\frac{\mathrm{d}H}{\mathrm{d}X} + \frac{\mathrm{d}P_\infty}{\mathrm{d}X}\right)\right] + \frac{4}{H} = 0. \tag{5.3}$$

5.2. *Matching between the thermal boundary layer and the bulk fluid*

The required behaviour of the solution in the thermal boundary layer as $Z \to \infty$ depends on whether or not there is a horizontal boundary within a certain distance below the heated plate.

If there is no such boundary, or if there is one at a (dimensional) distance much greater than $E^{-1}L$, then there is sufficient space for the Taylor–Proudman constraint

to be relaxed, and fluid can be drawn in without a significant pressure gradient. Consequently, we can write $P_\infty(X) = 0$ and $P_0 = H$. We then obtain an equation for $H(X)$:

$$\frac{1}{X^\ell}\frac{\mathrm{d}}{\mathrm{d}X}\left(X^\ell \frac{\mathrm{d}H}{\mathrm{d}X}\right) + \frac{4}{H} = 0. \tag{5.4}$$

With knowledge of $H(X)$, and hence of $P_0(X)$ and $P_\infty(X)$, the full solution may be recovered from (3.6)–(3.9) and (4.6)–(4.10).

If there is a lower boundary at $Z = Z^*$, with $1 \ll Z^* \ll Ra^{1/2}E^{-1/4}$ (i.e. greater than the thickness of the thermal boundary layer, and less than Taylor adjustment length), then a second Ekman layer forms above it. By analogy with (3.9), the horizontal pressure gradient as $Z \to Z^*$ is coupled to the vertical velocity $W = -1/H$ that persists from the thermal boundary layer by

$$W(X, Z^*) = -\frac{1}{4X^\ell}\frac{\mathrm{d}}{\mathrm{d}X}\left(X^\ell \frac{\mathrm{d}P_\infty}{\mathrm{d}X}\right) = -\frac{1}{H}. \tag{5.5}$$

Combining this with (5.3), we find that

$$P_\infty(X) = -\tfrac{1}{2}H(X), \qquad P_0(X) = \tfrac{1}{2}H(X), \tag{5.6}$$

and the equation for $H(X)$ is now

$$\frac{1}{X^\ell}\frac{\mathrm{d}}{\mathrm{d}X}\left(X^\ell \frac{\mathrm{d}H}{\mathrm{d}X}\right) + \frac{8}{H} = 0. \tag{5.7}$$

With the amended expressions (5.6) for P_0 and P_∞, the full solution can be recovered from (3.6)–(3.9) and (4.6)–(4.10) as before.

The net effect of a bottom boundary is to halve the effective pressure gradient from the thermal field that acts on the upper Ekman layer, so that an equal but opposite pressure gradient can act on the lower Ekman layer to balance the vertical fluxes. The thermal boundary layer is then an adjustment region from anticyclonic circulation close to the upper Ekman layer to cyclonic circulation that matches with the interior flow (and thence to the lower Ekman layer). We shall not concern ourselves further with the case of a lower boundary, since the transformation $H \mapsto \sqrt{2}H$ can be used to obtain the solution of (5.7) from that of (5.4).

6. Solution for $H(X)$

Equation (5.4) is subject to the symmetry ($\ell = 0$) or regularity ($\ell = 1$) condition $H'(0) = 0$, and some kind of boundary condition at the plate edge $X = 1$. Since (5.4) is invariant under the transformation $(X, H) \mapsto (\alpha X, \alpha H)$, the solution is of the form

$$H(X) = H(0)\,\Phi(X/H(0)), \tag{6.1}$$

where $\Phi(X)$ is the solution of (5.4) with $\Phi(0) = 1$ and $\Phi'(0) = 0$.

For the planar strip ($\ell = 0$) there is an analytic solution

$$\Phi(\xi) = \exp\{-[\mathrm{erf}^{-1}(\xi\sqrt{8/\pi})]^2\}. \tag{6.2}$$

For the axisymmetric disk ($\ell = 1$), the most we can obtain analytically is a series expansion

$$\Phi(\xi) = 1 - \xi^2 - \frac{1}{4}\xi^4 - \frac{5}{36}\xi^6 - \cdots \tag{6.3}$$

about $\xi = 0$, which must be extended numerically.

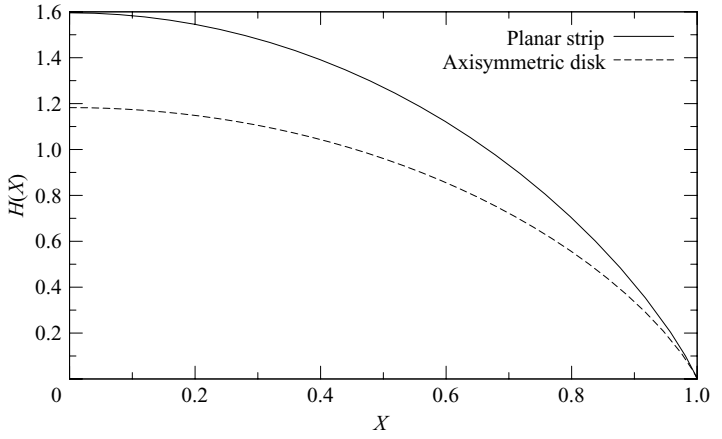

FIGURE 3. Solutions to equation (5.4) for the dimensionless thickness H of the thermal boundary layer as a function of the dimensionless horizontal coordinate X.

In both cases, we find that $\Phi(\xi) \to 0$ and $\Phi'(\xi) \to \infty$ as $\xi \to \xi_0$, where $\xi_0 = (\pi/8)^{1/2}$ ($\ell = 0$) or $\xi_0 = 0.845$ ($\ell = 1$). As shown in § 7, the plate edge $X = 1$ corresponds (at least to leading order) to the singularity at $\xi = \xi_0$. From this we deduce that $H(0) = 1.596$ ($\ell = 0$) or 1.183 ($\ell = 1$).

The solutions for $H(X)$ are shown in figure 3. Once $H(X)$ is known, the full solution for the fluid velocity and temperature can then be recovered from (3.6)–(3.9) and (4.6)–(4.10) together with the scalings (2.11)–(2.15). As might be expected from the geometry, a disk drains more effectively than a strip, in the sense that $H(X)$ is smaller for a disk.

7. Flow over the plate edge

In the solution described above,

$$H(X) \sim (X_0 - X)[-8\ln(X_0 - X)]^{1/2} \quad \text{and} \quad H'(X) \sim [-8\ln(X_0 - X)]^{1/2} \qquad (7.1)$$

as $X \to X_0$, where $X = X_0 \approx 1$ is the location of the singularity of (5.4). The divergence of H^{-1} and H' implies a divergence of the velocities in (3.8), (3.9) and (4.7)–(4.10), and also of the heat flux from (3.6). Many of these divergences are only logarithmic, but they indicate that the flow over the edge of the plate must be in a different dynamic regime from that which governs the boundary-layer structure below the rest of the plate. In order to calculate the asymptotic form of the total heat flux, we need to examine the flow structure near the edge.

7.1. *Asymptotic structure near the edge*

Close to the plate edge, the thickness of the thermal boundary layer may become much less than the fixed Ekman scale $\delta_E = LE^{-1/2}$. Rotational effects would then be negligible and the flow would be in the same regime as that studied by Higuera (1993). We also expect the gradient of the thermal boundary-layer thickness to become $O(1)$ as the corner is approached, at which point the fully two-dimensional equations must be used instead of boundary-layer approximations. However, as shown below, the flow does not pass directly from the solution of §§ 3–6 into either of these new regimes.

We estimate where the asymptotic approximations employed in §§ 3 and 4 cease to apply by substituting the solution obtained for the plate interior into the full

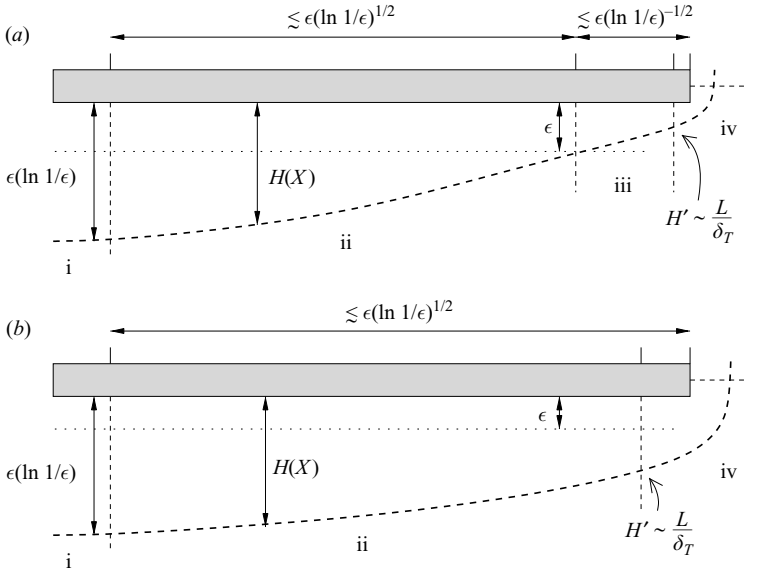

FIGURE 4. The two possible sequences of asymptotic regions near the plate edge: (i) interior, (ii) transition, (iii) 'non-rotating' boundary layer, and (iv) corner. The lengths are shown in terms of the dimensionless coordinates X and Z (see (2.11)), and $\epsilon = Ra^{1/2}E^{5/4} \ll 1$. The unscaled slope of the thermal boundary layer is $\mathrm{d}h/\mathrm{d}x = (\delta_T/L)\,\mathrm{d}H/\mathrm{d}X$.

equations (2.1)–(2.5) and examining the size of the neglected terms. We find that the approximations break down first in the thermal boundary layer as $X \to X_0$, owing to one of two sets of terms.

The first set relates to the growth of the ageostrophic velocity U_a as $X \to X_0$. As a result of this growth, U_a can no longer be neglected in (4.1) and horizontal advection can no longer be neglected in (4.3) and (4.5). These terms become significant when

$$\frac{H}{H'^2} \sim Ra^{1/2}E^{5/4} \Rightarrow (X_0 - X) \sim Ra^{1/2}E^{5/4}\left(\ln Ra^{-1/2}E^{-5/4}\right)^{1/2}. \tag{7.2}$$

The second set relates to the growth of horizontal gradients as $X \to X_0$. Horizontal diffusion becomes comparable with vertical diffusion in (4.3) and (4.5) when

$$H'^2 \sim Ra\,E^{3/2} \Rightarrow (X_0 - X) \sim \exp\left(-8Ra\,E^{3/2}\right). \tag{7.3}$$

From (2.17), both of these possibilities imply that $X_0 - X \ll 1$, and the exponentially small factor in (7.3) makes it likely that (7.2) is attained first. We assume this to be the case, and define $\epsilon = Ra^{1/2}E^{5/4} \ll 1$. The end of the interior regime thus corresponds to the breakdown of geostrophy in the thermal boundary layer.

The previously calculated solution below the interior of the plate, region (i) in figure 4, applies until

$$(X_0 - X) \sim \epsilon[\ln(1/\epsilon)]^{1/2} \Rightarrow H \sim \epsilon\ln(1/\epsilon), \quad H' \sim [\ln(1/\epsilon)]^{1/2}. \tag{7.4}$$

At this point, the thickness of the thermal boundary layer is still much greater than the $O(\epsilon)$ thickness of the Ekman layer, and the unscaled slope $\mathrm{d}h/\mathrm{d}x$ is still small. We therefore anticipate a transitional region (ii) in which rotational effects are still important and boundary-layer approximations still apply. This transition region

continues until either

$$H \sim \frac{\delta_E}{\delta_T} = \epsilon \qquad \text{or} \qquad \frac{\mathrm{d}H}{\mathrm{d}X} \sim \frac{L}{\delta_T} = Ra^{1/2}E^{-3/4}. \tag{7.5}$$

These conditions correspond respectively to rotational effects ceasing to be leading order, and to the slope of the thermal boundary layer becoming $O(1)$. As outlined in Appendix, the Prandtl number controls which condition is met first (larger Pr favours the first case).

In the first case there is a further region (iii) in which the unscaled slope $\mathrm{d}h/\mathrm{d}x$ of the thermal boundary layer is still small, and the flow is described by the non-rotating boundary-layer equations. When the slope becomes $O(1)$, the fluid enters a final region (iv) in which it turns the corner and rises round the edge of the plate. These regions are as shown in figure 4(a). Higuera (1993) analysed the singularity at the edge of a heated plate in a non-rotating system, and obtained solutions applicable to regions (iii) and (iv). In the second case, region (ii) matches directly to the corner region (iv), as shown in figure 4(b), and rotational effects also play a role in region (iv).

The horizontal pressure gradient driving the flow is proportional to the gradient of the thermal boundary-layer thickness H, and the outward mass flux is an increasing function of X owing to the vertical upflow W. It is therefore reasonable to assume that in regions (ii)–(iv) H' remains at least as large as the $O([\ln 1/\epsilon]^{1/2})$ value at the outer edge of region (i). With the transition heights given by (7.4) and (7.5), this assumption about H' sets upper bounds on the (dimensionless) lengths of these regions: $O(\epsilon[\ln 1/\epsilon]^{1/2})$ for region (ii) and $O(\epsilon[\ln 1/\epsilon]^{-1/2})$ for regions (iii) and (iv). Regions (ii)–(iv) are therefore all short compared with the total length of the plate. Since the transition from the interior region (i) occurs at a distance $O(\epsilon[\ln 1/\epsilon]^{1/2})$ before the singularity at $X = X_0$, and since regions (ii)–(iv) are also at most this length, we deduce that $|1 - X_0| = O(\epsilon[\ln 1/\epsilon]^{1/2})$. Therefore it was indeed appropriate to set the singularity to coincide with the plate edge when calculating the leading-order interior solution in § 6.

7.2. *The total heat flux*

We turn now to calculation of the heat flux from the plate, for which the usual dimensionless expression is the Nusselt number. We define this by

$$Nu = -\frac{1}{L^\ell \Delta T}\int_0^L x^\ell \left.\frac{\partial T}{\partial z}\right|_{z=0} \mathrm{d}x = -Ra^{1/2}E^{3/4}\int_0^1 X^\ell \left.\frac{\partial \theta}{\partial Z}\right|_{Z=0} \mathrm{d}X\,. \tag{7.6}$$

The contribution Nu_{i} to the heat flux from region (i) is found by integrating the solution from § 6 over most of the plate. Substituting from (4.6) and making use of (5.4), we obtain

$$Nu_{\mathrm{i}} \sim Ra^{1/2}E^{3/4}\int_0^{X_0-\epsilon(\ln 1/\epsilon)^{1/2}} \frac{X^\ell}{H}\,\mathrm{d}X \sim 2^{-1/2}Ra^{1/2}E^{3/4}[\ln(1/\epsilon)]^{1/2}\,. \tag{7.7}$$

An upper bound on the order of magnitude of the heat flux Nu_{ii} from region (ii) of the plate is obtained from a thermal boundary layer that decreases linearly in thickness from $O(\epsilon \ln 1/\epsilon)$ to $O(\epsilon)$ over a distance $O(\epsilon[\ln 1/\epsilon]^{1/2})$. Computing the appropriate integral, we find that

$$Nu_{\mathrm{ii}} \lesssim Ra^{1/2}E^{3/4}\frac{\ln[\ln(1/\epsilon)]}{[\ln(1/\epsilon)]^{1/2}} \ll Nu_{\mathrm{i}} \tag{7.8}$$

For the case where region (iii) exists, we match the heat and mass fluxes and the layer height to the solution presented by Higuera (1993) for a non-rotating plate (see Appendix for details). The total heat flux in Higuera's solution is dominated by the heat flux from the interior of the plate rather than that from the singularity near the edge. We find that regions (iii) and (iv) correspond to only a small end-region of Higuera's solution, and hence that the heat-flux contribution is small compared with the flux $Nu_{\rm ii} + Nu_{\rm i}$ entering from region (ii). Hence $Nu_{\rm iii} + Nu_{\rm iv} \ll Nu_{\rm i}$. For the case where region (iii) does not appear, the flux from region (iv) is included in the estimate of $Nu_{\rm ii}$, since the thermal boundary layer H remains thicker than $O(\epsilon)$.

In all cases, we conclude that the total heat flux is dominated by the contribution $Nu_{\rm i}$ from the interior region, and hence that

$$Nu \sim 2^{-1/2} Ra^{1/2} E^{3/4} \left[\ln \left(Ra^{-1/2} E^{-5/4} \right) \right]^{1/2}. \tag{7.9}$$

The main algebraic part of this scaling originates from $\delta_T / L = Ra^{-1/2} E^{-3/4}$ and is associated with the confinement of the thermal boundary layer by Ekman suction. The logarithmic factor arises from a further enhancement due to the singularity as the plate edge is approached.

8. Uniform-heat-flux boundary condition

In §§ 3–7, we described the solution for a uniform plate temperature. The other canonical boundary condition is that of uniform heat flux. The problem is then characterized by a total heat flux (say $2Q$ for the strip and πQ for the disk), rather than a temperature difference ΔT. We now need to determine the temperature of the plate as part of the solution.

The analysis for a uniform heat flux is quite similar to that for a uniform temperature, and we are able to re-use the scalings of § 2.2 by setting

$$\Delta T = \frac{Q \, \delta_T}{k \, L^{1+\ell}} \tag{8.1}$$

in (2.6) and (2.15), where k is the thermal conductivity of the fluid. The thermal boundary condition on the plate is then $\partial \theta / \partial Z = -1$ rather than $\theta = 1$.

The main difference in the analysis is that it is necessary to keep $\theta_0(X)$ as an extra independent variable, since the temperature in the Ekman layer is unknown at the outset. Integrating (3.5) across the Ekman layer, we obtain a boundary condition on the temperature gradient at the top of the thermal boundary layer in the form

$$\left. \frac{\partial \theta}{\partial Z} \right|_{Z \to 0} = -1 + \frac{\mathrm{d}\theta_0}{\mathrm{d}X} \int_0^\infty U \, \mathrm{d}\zeta. \tag{8.2}$$

Following the previous analysis, we then obtain a pair of equations governing the behaviour of the solution. The direct analogue of (5.4) is

$$\frac{1}{X^\ell} \frac{\mathrm{d}}{\mathrm{d}X} \left(X^\ell \frac{\mathrm{d}(\theta_0 H)}{\mathrm{d}X} \right) + \frac{4}{H} = 0, \tag{8.3}$$

and we also have a new equation

$$\frac{\theta_0}{H} = 1 + \frac{1}{4} \frac{\mathrm{d}(\theta_0 H)}{\mathrm{d}X} \frac{\mathrm{d}\theta_0}{\mathrm{d}X}, \tag{8.4}$$

which results from the application of (8.2) to the temperature profile (4.6).

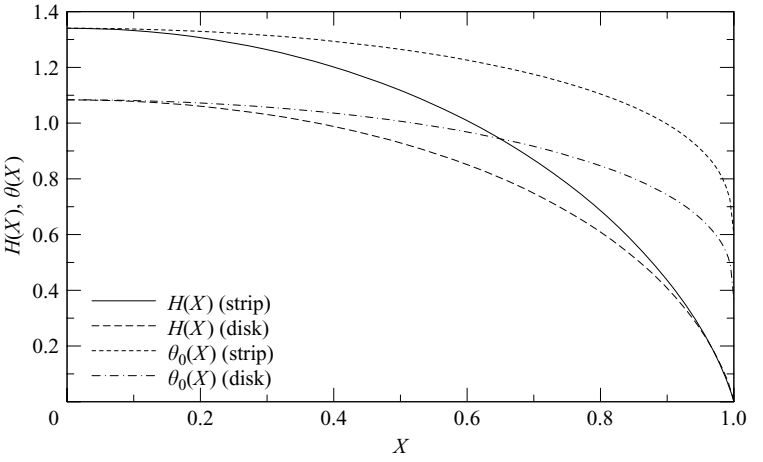

FIGURE 5. The dimensionless thickness H of the thermal boundary layer and the dimensionless temperature θ_0 of the plate as functions of the horizontal coordinate X for the case of a uniform heat flux.

The boundary conditions on (8.3) and (8.4) are $\theta_0'(0) = H'(0) = 0$ from symmetry or regularity and $H(1) = 0$ from matching at the plate edge. Invariance under the transformation $(X, H, \theta_0) \mapsto (\alpha^3 X, \alpha^2 H, \alpha^2 \theta_0)$ allows the solution again to be obtained by rescaling a single integration from $X = 0$. The thickness H of the thermal boundary layer and temperature θ_0 of the plate are plotted in figure 5.

In this case the heat flux near $X = 1$ is necessarily finite, but the layer thickness still goes to zero and the mass flux diverges. This singularity (identified with the plate edge) exhibits the local behaviour

$$H(X) \sim (1 - X)[36(1 + \ell)]^{1/3}[-\ln(1 - X)]^{2/3}, \tag{8.5}$$

$$\theta_0(X) \sim \left[\frac{4}{3(1 + \ell)^2}\right]^{1/3} [-\ln(1 - X)]^{-1/3}. \tag{8.6}$$

As before, short correction regions must be introduced to regularize the flow in the neighbourhood of the corner, but these do not affect the leading-order solution under the interior of the plate.

9. Conclusions

We have calculated asymptotic solutions for the Ekman and thermal boundary-layer structures beneath a horizontal heated plate in a rapidly rotating system. For $E^{-3/2} \ll Ra \ll E^{-5/2}$ the lateral drainage of hot fluid occurs primarily in the Ekman layer, while the thermal boundary layer is much thicker than the Ekman layer and confined by Ekman suction. The details of the breakdown of this structure near the edge of the plate do not affect the solution under the plate at leading order, but simply serve to impose a boundary condition of zero boundary-layer thickness at the edge. In some sense this is fortunate since the details of the breakdown (figure 4) are delicate and involve subregions that differ only logarithmically from each other.

In addition to the structure of the solution, the main results are the heat flux from a plate held at a fixed temperature and the temperature distribution on a plate maintained with a uniform heat flux, which are calculated for both a strip and a disk. In the fixed-temperature problem, the asymptotic scaling (7.9) for the Nusselt

number (including the numerical pre-factor) applies to both geometries, which might initially be surprising. However, this can be understood from the fact that the dominant contribution to the heat transfer is due to the logarithmic singularity (7.1) in the boundary-layer solution as the fluid nears the plate edge. This singularity is independent of the geometry, and the scalings employed are such that the length of the plate edge (in the y-direction) appears equivalent in the two geometries.

The main algebraic part of the Nusselt-number scaling (7.9) originates from the thermal boundary-layer scaling $\delta_T/L \sim Ra^{-1/2}E^{-3/4}$ under the plate. Comparing the Nusselt-number scaling with the $Ra^{1/5}$ scaling that applies in the absence of rotation, we see that the rotation inhibits the convection by a factor of approximately $(Ra^{1/2}E^{5/4})^{3/5} \ll 1$. Thus the rotation, and specifically the confinement of the outflow to a thin Ekman layer, significantly reduces the overall heat transfer.

An interesting question is whether the rotational constraint could be broken by instability and unsteadiness in the flow. Small-scale instability and turbulence could lead, as is common in geophysical flows, to effective enhancement of the molecular diffusivities ν and κ, but need not qualitatively change the overall solution structure. Large-scale baroclinic instability, such as that that seen, for example, on the edges of coastal currents or localized free-surfaces vortices (e.g. Griffiths & Linden 1981*a*, *b*), might lead to horizontal eddies on the $O(Ra^{1/4}E^{5/8}Pr^{-1/2}L)$ scale of the Rossby radius in the thermal boundary layer and contribute to the lateral heat transport. However, baroclinic instability is unlikely without a second boundary below the plate, thermal diffusion and Ekman suction are stabilizing influences, and steady flow was observed in the top-heated rotating experiments of Pedlosky *et al.* (1997). Given the uncertainty, it would be desirable in future work to examine the stability of the steady flows described above, either through numerical stability analysis of perturbations about the steady solutions that are harmonic in y and t or through experimental investigations.

Finally, we note that, while we have solved here two particular problems with uniform boundary conditions, the method for the interior solution is more widely applicable. It would now be relatively straightforward to produce steady solutions for any imposed temperature, or heat-flux conditions.

Appendix. Matching up to the corner region

In the non-rotating version of the heated-plate problem (studied by Higuera 1993, and many others) there are well-defined scales for the (dimensional) horizontal mass flux q and thermal boundary-layer thickness h. For an infinite strip of width $2\widehat{L}$, with corresponding Rayleigh number $\widehat{Ra}$, it is found that

$$h = \widehat{L}\widehat{Ra}^{-1/5} f(\eta), \quad q = \kappa \widehat{Ra}^{1/5} g(\eta), \tag{A 1}$$

where $\eta = \widehat{x}/\widehat{L}$ is the scaled horizontal distance from the centre of the strip. The functions f and g are $O(1)$ over most of the strip (with the obvious exception that $g(\eta) \to 0$ at the centre). Higuera (1993) examined the singularity at the edge of the plate, and showed that $f(\eta) \sim (1-\eta)^{1/4}$ in $\widehat{Ra}^{-1/5} \ll 1-\eta \ll 1$ for $Pr \gg 1$, whereas $f(\eta)$ remains $O(1)$ with $f' \to \infty$ as $\eta \to 1$ for $Pr = O(1)$. In both cases there is a final region, analogous to region (iv) in figure 4, corresponding to flow round the plate corner.

Returning to the rotating problem, the matching between the transition region (ii) of figure 4 and a non-rotating boundary layer (iii) should occur where

$$h \sim LE^{1/2}, \quad q \sim \kappa Ra^{1/2}E^{3/4}\left(\ln Ra^{-1/2}E^{-5/4}\right)^{1/2}. \tag{A 2}$$

Comparison of these values with those from the non-rotating solution yields the effective length $\widehat{L}$ and matching point η^*. By examining the ratio q^2/h^3 to eliminate $\widehat{L}$, we obtain

$$\frac{g^2}{f^3} \sim \left(\ln Ra^{-1/2}E^{-5/4}\right)^{1/2} \gg 1. \tag{A 3}$$

For $Pr \gg 1$ this implies that $(1-\eta^*) \ll 1$ (i.e. region (iii) corresponds to only the outermost part of the non-rotating solution). For $Pr = O(1)$ the matching condition (A 3) cannot be satisfied, which suggests that the quasi-parallel-flow condition $\mathrm{d}h/\mathrm{d}x$ must break down before $H \sim \epsilon$. In other words, region (ii) ends with a rotating analogue of the singularity in slope identified by Higuera (1993), and region (ii) matches directly to the corner region (iv) in which $\partial h/\partial x = O(1)$. In either case, the details of the flow in these end regions affect neither the leading-order heat transfer nor the flow structure and temperature distribution under most of the plate, and hence they will not be investigated further here.

REFERENCES

Aihara, T., Yamada, Y. & Endo, S. 1972 Free convection along the downward-facing surface of a heated horizontal plate. *Intl J. Heat Mass Transfer* **15**, 2535–2549.

Bloxham, J. & Gubbins, D. 1987 Thermal core–mantle interactions. *Nature* **325**, 511–513.

Boubnov, B. M. & Fernando, H. J. 1999 Regimes of convection from an isolated buoyancy source in a rotating fluid. *Izv. Atmos. Ocean. Phys.* **35**, 440–448.

Busse, F. H. 1970 Thermal instabilities in rapidly rotating systems. *J. Fluid Mech.* **44**, 441–460.

Dormy, E., Soward, A. M., Jones, C. A., Jault, D. & Cardin, P. 2003 The onset of thermal convection in rotating spherical shells. *J. Fluid Mech.* **501**, 43–70.

Gibbons, S. J. & Gubbins, D. 2000 Convection in the Earth's core driven by lateral variations in the core–mantle boundary heat flux. *Geophys. J. Intl* **142**, 631–642.

Goldstein, R. J. & Lau, K.-S. 1983 Laminar natural convection from a horizontal plate and the influence of plate-edge extensions. *J. Fluid Mech.* **129**, 55–75.

Griffiths, R. W. & Linden, P. F. 1981*a* The stability of buoyancy-driven coastal currents. *Dyn. Atmos. Oceans* **5**, 281–306.

Griffiths, R. W. & Linden, P. F. 1981*b* The stability of vortices in a rotating, stratified fluid. *J. Fluid Mech.* **105**, 283–316.

Hatfield, D. W. & Edwards, D. K. 1981 Edge and aspect ratio effects in natural convection from the horizontal heated plate facing downwards. *Intl J. Heat Mass Transfer* **24**, 1019–1024.

Higuera, F. J. 1993 Natural convection below a downward facing horizontal plate. *Eur. J. Mech.* B/*Fluids* **12**, 289–311.

Hunter, C. 1967 The axisymmetric flow in a rotating annulus due to a horizontally applied temperature gradient. *J. Fluid Mech.* **27**, 753–778.

Jones, C. A., Soward, A. M. & Musse, A. I. 2000 The onset of thermal convection in a rapidly rotating sphere. *J. Fluid Mech.* **405**, 157–179.

Kohler, M. D. & Stevenson, D. J. 1990 Modelling core-fluid motions and the drift of magnetic field patterns at the CMB by use of topography obtained by seismic inversion. *Geophys. Res. Lett.* **17**, 1473–1476.

Labrosse, S., Poirier, J. P. & Le Mouël, J. L. 1997 On cooling of the Earth's core. *Phys. Earth Planet. Inter.* **99**, 1–17.

Lister, J. R. 2004 Thermal winds forced by inhomogeneous boundary conditions in rotating, stratified, hydromagnetic fluid. *J. Fluid Mech.* **505**, 163–178.

Lister, J. R. & Buffett, B. A. 1998 Stratification of the outer core at the core–mantle boundary. *Phys. Earth Planet. Inter.* **105**, 5–19.

McIntyre, M. E. 1968 The axisymmetric convective regime for a rigidly bounded rotating annulus. *J. Fluid Mech.* **32**, 625–655.

Olson, P. & Christensen, U. R. 2002 The time-averaged magnetic field in numerical dyanmos with non-uniform boundary heat flow. *Geophys. J. Intl* **151**, 809–823.

Olson, P. & Glatzmaier, G. A. 1996 Magnetoconvection and thermal coupling of the Earth's core and mantle. *Phil. Trans. R. Soc. Lond.* A **354**, 1413–1424.

Pedlosky, J., Whitehead, J. A. & Veitch, G. 1997 Thermally driven motions in a rotating stratified fluid: Theory and experiment. *J. Fluid Mech.* **339**, 391–411.

Roberts, P. H. 1968 On the thermal instability of a rotating fluid sphere containinng heat sources. *Phil. Trans. R. Soc. Lond.* A **263**, 93–117.

Sarson, G. R., Jones, C. A. & Longbottom, A. W. 1997 The influence of boundary region heterogeneities on the geodynamo. *Phys. Earth Planet. Inter.* **101**, 13–32.

Singh, S. N. & Birkebak, R. C. 1969 Laminar free convection from a horizontal infinite strip facing downwards. *Z. Angew. Math. Phys.* **20**, 454–461.

Zhang, K. & Gubbins, D. 1992 On convection in the Earth's core driven by lateral temperature variations in the lower mantle. *Geophys. J. Intl* **108**, 247–255.